Electronic supplementary information

Regioselective C–H hydroxylation of *n*-alkanes using Shilov-type Pt catalysis in perfluorinated micro-emulsions

*Michiel Janssen and Dirk E. De Vos**

Centre for Membrane Separations, Adsorption, Catalysis and Spectroscopy for Sustainable Solutions (cMACS), KU Leuven, Celestijnenlaan 200F, 3001 Leuven, Belgium.

*E-mail: dirk.devos@kuleuven.be

1 Experimental

a) Product analysis and identification

As described in the experimental section of the main manuscript, non-polar high molecular weight products, as well as higher aliphatic carboxylic acids, were analyzed by gas chromatography (GC), while proton nuclear magnetic resonance (^{1}H NMR) spectroscopy was conducted to detect possibly formed polar low molecular weight compounds.

GC

After extraction of the aqueous product mixture with chloroform ($CHCl_3$), the resulting organic phase was analyzed by GC before and after derivatization with *N*,*O*-bis(trimethylsilyl)-trifluoroacetamide (BSTFA; 54 µL, 90 min, 60 °C, 500 rpm), using a DB-FFAP and CP-Sil 5 CB column, respectively. For a standard reaction (150 °C, 1 h, 20 bar O_2) of *n*-heptane with K_2PtCl_4 (1 mol%) as catalyst and perfluorooctanoic acid (PFOA; 0.48 M) as surfactant, representative chromatograms are displayed in Figures S1, S2 and S3. The identity of each peak was confirmed by comparing its retention time with that obtained for a commercial or synthesized sample.

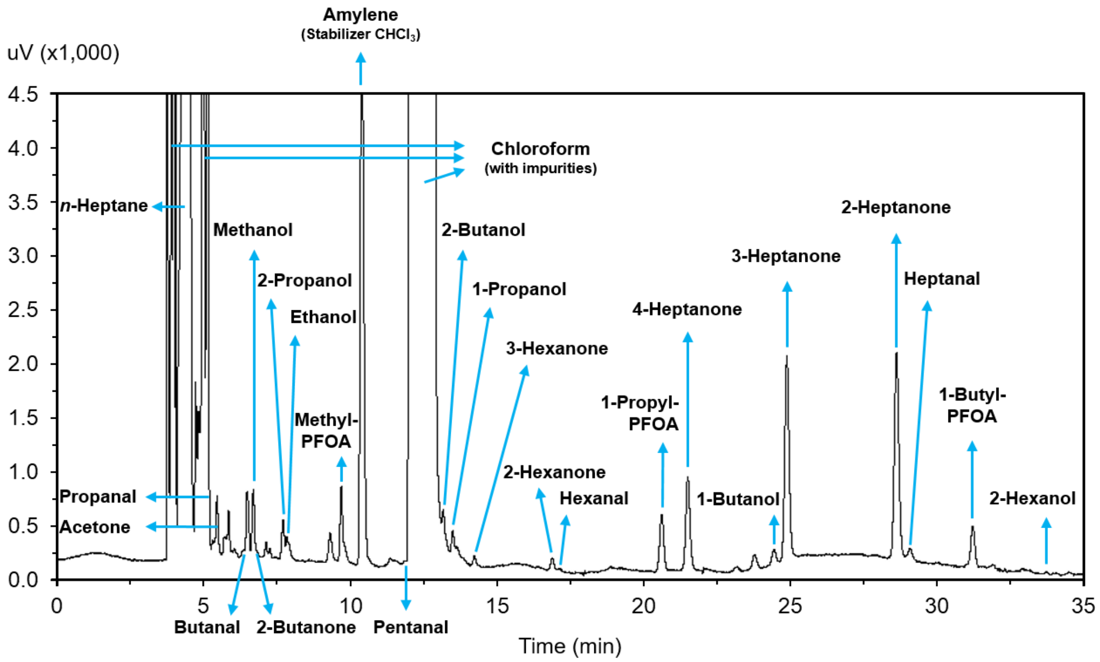

Figure S1. Gas chromatogram with annotated peaks of a sample taken after 1 h in the Pt^{II}-catalyzed oxidation of *n*-heptane in a perfluorinated micro-emulsion, displayed for retention times between 0 and 35 min. Conditions: *n*-heptane (0.67 M), K_2PtCl_4 (1 mol%), H_2SO_4 (0.33 M), perfluorooctanoic acid (PFOA; 0.48 M), H_2O (1.5 mL), 1 h, 150 °C, 20 bar O_2.

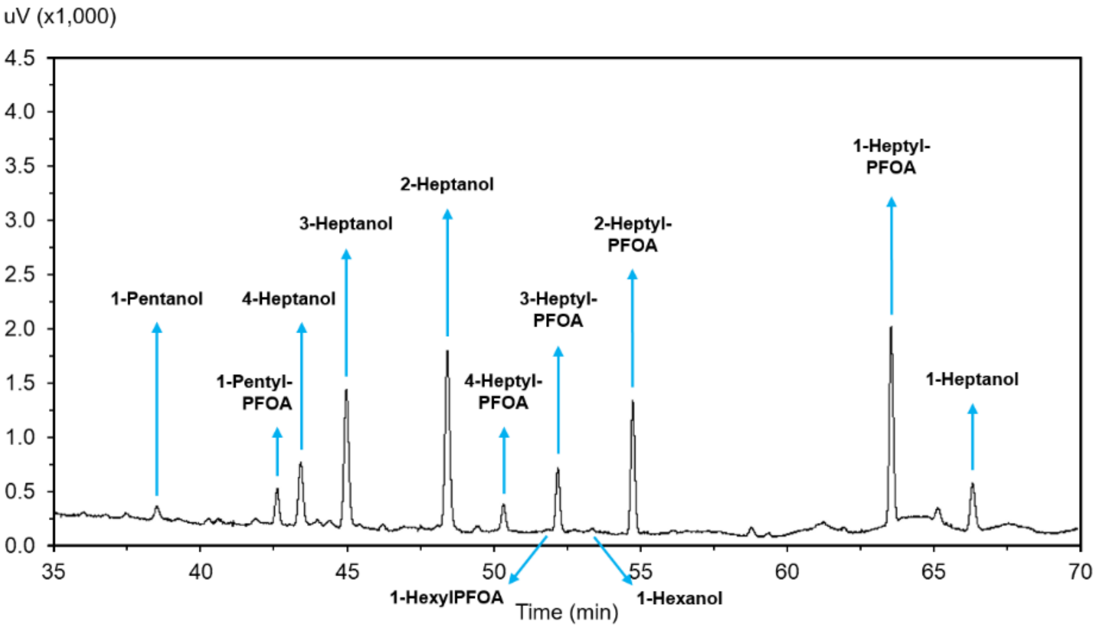

Figure S2. Gas chromatogram with annotated peaks of a sample taken after 1 h in the Pt^{II}-catalyzed oxidation of *n*-heptane in a perfluorinated micro-emulsion, displayed for retention times between 35 and 70 min. Conditions: *n*-heptane (0.67 M), K_2PtCl_4 (1 mol%), H_2SO_4 (0.33 M), perfluorooctanoic acid (PFOA; 0.48 M), H_2O (1.5 mL), 1 h, 150 °C, 20 bar O_2.

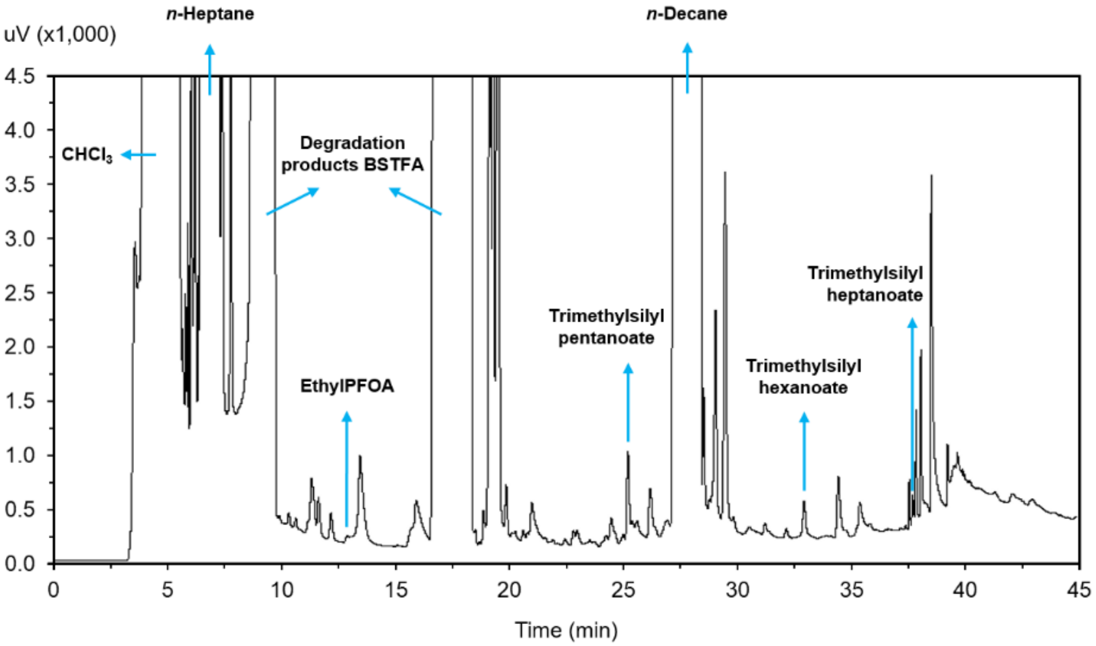

Figure S3. Gas chromatogram of a sample taken after 1 h in the Pt^{II}-catalyzed oxidation of *n*-heptane in a perfluorinated micro-emulsion and subjected to derivatization with *N*,*O*-bis(trimethylsilyl)trifluoroacetamide (BSTFA). For clarity, compounds already displayed in Figures S1 and S2 are not annotated. Conditions: *n*-heptane (0.67 M), K_2PtCl_4 (1 mol%), H_2SO_4 (0.33 M), perfluorooctanoic acid (PFOA; 0.48 M), H_2O (1.5 mL), 1 h, 150 °C, 20 bar O_2. Silylation: 300 µL $CHCl_3$-phase, 54 µL BSTFA, 90 min, 60 °C, 500 rpm.

^{1}H NMR

In general, each NMR spectrum was calibrated before data analysis by an automatic baseline correction and by positioning the singlet signal of benzyl alcohol (external standard) at 4.65 ppm.[1] Abbreviations used to designate multiplicities include: s = singlet, d = doublet, t = triplet, q = quartet, quin = quintet, m = multiplet. In addition, chemical shifts (δ) and coupling constants (J) are expressed in ppm and Hz, respectively. The following products were identified:

Methanol (MW = 32 g/mol)

^{1}H NMR (400 MHz; D_2O): δ_H 3.38 (3 H, s, C**H**$_3$-).

Formic acid (MW = 46 g/mol)

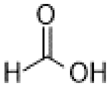

^{1}H NMR (400 MHz; D_2O): δ_H 8.36 (1 H, s, **H**-COOH).

Ethanol (MW = 46 g/mol)

^{1}H NMR (400 MHz; D_2O): δ_H 3.67 (2 H, q, *J* = 7.0, CH_3-C**H**$_2$-OH), 1.20 (3 H, t, *J* = 7.0, C**H**$_3$-CH_2-OH).

Acetaldehyde (MW = 44 g/mol)

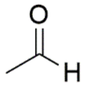

^{1}H NMR (400 MHz; D_2O): δ_H 9.69 (1 H, s, CH_3-CO-**H**), 2.24 (3 H, s, C**H**$_3$-CO-H).

Acetic acid (MW = 60 g/mol)

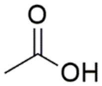

^{1}H NMR (400 MHz; D_2O): δ_H 2.10 (3 H, s, C**H**$_3$-COOH).

Glycolic acid (MW = 76 g/mol)

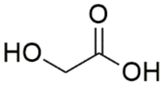

^{1}H NMR (400 MHz; D$_2$O): δ_H 4.16 (2 H, s, HO-C**H**$_2$-COOH).

Propionic acid (MW = 74 g/mol)

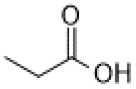

^{1}H NMR (400 MHz; D$_2$O): δ_H 2.40 (2 H, q, *J* = 7.5, CH$_3$-C**H**$_2$-COOH), 1.10 (3 H, t, *J* = 7.5, C**H**$_3$-CH$_2$-COOH).

Lactic acid (MW = 90 g/mol)

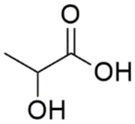

^{1}H NMR (400 MHz; D$_2$O): δ_H 4.33 (1 H, q, *J* = 6.8, CH$_3$-C**H**(-OH)-COOH), 1.42 (3 H, d, *J* = 6.8, C**H**$_3$-CH(-OH)-COOH).

Butyric acid (MW = 88 g/mol)

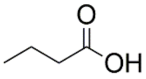

^{1}H NMR (400 MHz; D$_2$O): δ_H 2.35 (2 H, t, *J* = 7.3, -CH$_2$-C**H**$_2$-COOH), 1.61 (2 H, m, *J* = 7.3, CH$_3$-C**H**$_2$-CH$_2$-), 0.93 (3 H, t, *J* = 7.3, C**H**$_3$-CH$_2$-).

b) Product grouping

The compounds identified during qualitative analysis were grouped based on their molecular structure. More specifically, different categories were constructed according to (i) the corresponding carbon number and (ii) the presence of a particular functional group. As a result, following eight product classes were distinguished:

- C_7 Alcohols ($C_7(OH)$): 1-heptanol, 2-heptanol, 3-heptanol, 4-heptanol;
- C_7 Ketones ($C_7(O)$): 2-heptanone, 3-heptanone, 4-heptanone;
- C_7 Aldehyde ($C_7H(O)$): heptanal;
- C_7 Acid ($C_6(COOH)$): heptanoic acid;
- Lower alcohols ($\leq C_6(OH)$); methanol, ethanol, 1-propanol, 1-butanol, 1-pentanol, 1-hexanol, 2-propanol, 2-butanol, 2-hexanol;
- Lower ketones ($\leq C_6(O)$): acetone, 2-butanone, 2-hexanone, 3-hexanone;
- Lower aldehydes ($\leq C_6H(O)$): acetaldehyde, propanal, butanal, pentanal, hexanal;
- Lower carboxylic acids ($\leq C_5(COOH)$): formic acid, acetic acid, glycolic acid, propionic acid, lactic acid, butanoic acid, pentanoic acid, hexanoic acid.

A complete overview is given in Figure S4, with illustration of the corresponding molecular structures. Although not shown here, the C_7 alcohols and lower primary alcohols were present in both the free form and as ester with PFOA. Moreover, fragmentation of the primary oxidation products occurred during reaction, as a result of which product yields were corrected using the carbon number and denoted as carbon yields.

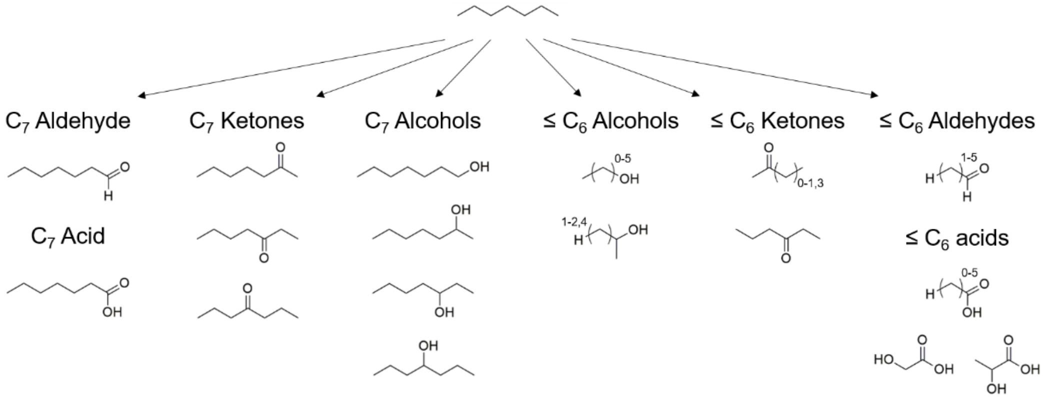

Figure S4. Product spectrum of the Pt^{II}-catalyzed oxidation of *n*-heptane in a perfluorinated micro-emulsion.

2 Pt-mediated alkane oxidation in perfluorinated micro-emulsions

a) Oxidation of cyclohexane

To evaluate the applicability of using a Pt^{II}-based perfluorinated micro-emulsion system for the selective hydroxylation of commercially available alkanes, cyclohexane was subjected to similar reaction conditions (1 h, 130 °C, 20 bar O_2) as those applied for the transformation of *n*-heptane. As illustrated by the results in Table S1, similar trends were observed. Notably, considerable conversion with high selectivity for cyclohexanol was exclusively obtained when both K_2PtCl_4 (1 mol%) and PFOA (0.48 M) were included in the acidic aqueous reaction mixture (0.33 M H_2SO_4). Accordingly, these results strongly support the original assumption that the formation of a micro-emulsion is essential to ensure efficient cooperation of the different reactants in solution and, hence, to obtain an active Shilov-inspired Pt^{II} system.

Table S1. Carbon yields in the Pt^{II}-catalyzed oxidation of cyclohexane in a perfluorinated micro-emulsion.[a]

Catalyst	Surfactant	C (%)	Carbon yield (%)[b]				
			CyOH[c]	CyO	ADPA	6-HHA	≤ C_4(COOH)
-	-	0.03	0	0	0	0	0.03
K_2PtCl_4	-	0.11	0.04	0.07	0	0	0.01
-	PFOA	0.85	0.25	0.25	0.12	0.19	0.04
K_2PtCl_4	PFOA	0.43	0.18	0.11	0.03	0.07	0.04

[a] Conditions: cyclohexane (0.67 M), K_2PtCl_4 (0-1 mol%), H_2SO_4 (0.33 M), perfluorooctanoic acid (PFOA; 0-0.48 M), H_2O (1.5 mL), 1 h, 130 °C, 20 bar O_2. Abbreviations: CyOH, cyclohexanol; CyO, cyclohexanone; ADPA, adipic acid; 6-HHA, 6-hydroxyhexanoic acid; ≤ C_4(COOH), lower mono- and dicarboxylic acids. [b] Number of mmoles of C in the respective product divided by the total mmoles of C initially supplied in cyclohexane (6 mmol). [c] Present in free form and as ester with PFOA.

b) Fate of radicals in a perfluorinated micro-emulsion

A significant rate enhancement was observed upon adding PFOA to a metal-free reaction mixture, which suggests that the fate of the radicals formed in a classic autoxidation might be different when the reaction is conducted in a perfluorinated medium, rather than in a bulk hydrocarbon solution. Additional insights were therefore gained by closely examining the selectivity patterns obtained after performing the oxidation in pure *n*-heptane vs. perfluorooctane at similar conversion (Figure S5). However, comparable selectivities were invariably observed for both systems, pointing towards nearly identical autoxidation reactions in which the radicals react in an analogous manner. Accordingly, the introduction of a perfluorinated micro-emulsion does not seem to alter the fate of the radicals formed during the oxidation of *n*-heptane.

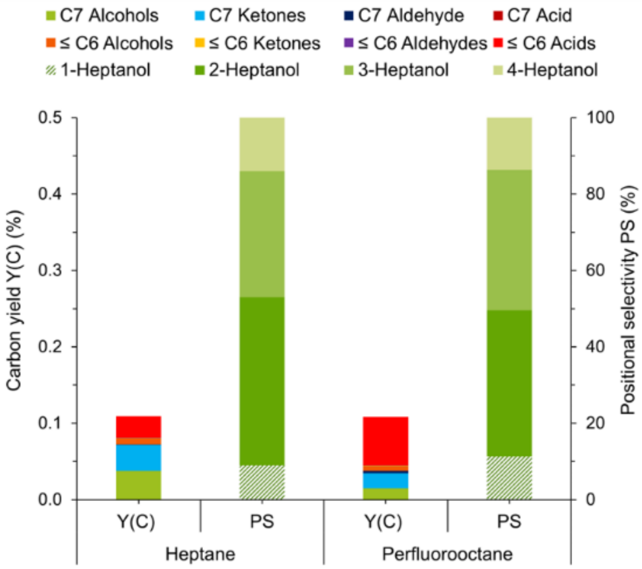

Figure S5. Autoxidation in pure *n*-heptane vs. perfluorooctane at similar conversion. Conditions: *n*-heptane (0.147-1 mL), perfluorooctane (1 mL), 1 h, 140 °C, 20 bar O_2.

3 Insight into the catalytic role of Pt^{II}

a) Transformation of 2,2,3,3-tetramethylbutane

To obtain additional evidence for the involvement of Pt^{II} in activating the highly inert primary C–H bonds of *n*-heptane, 2,2,3,3-tetramethylbutane (TMB) was subjected to identical standard reaction conditions (150 °C, 20 bar O_2). After 2 h, sample preparation was performed in a similar way as described for *n*-heptane, with subsequent analysis of the organic phase on an Agilent 6890 GC instrument, containing an HP-1 MS column and coupled to an Agilent 5973 MSD mass spectrometer. The latter is equipped with an electron impact ion source and a single quadrupole mass filter. From the resulting chromatogram (Figure S6), a distinct peak was visible at a retention time of 21.9 min; a thorough study of the corresponding fragmentation pattern revealed the formation of 2,2,3,3-tetramethyl-1-butyl perfluorooctanoate as sole reaction product (Figure S7). Particularly, fragments with an m/z ratio of 57 and 41 represent the basic molecular structure of TMB, i.e. a *tert*-butyl group, while peaks at m/z ratios of 369, 281, 231, 219, 181, 169, 131, 119 and 69 are in good agreement with the fragmentation pattern of PFOA, as reported in the NIST mass spectral database (NIST MS number: 231756), and thus, imply the presence of a perfluorinated aliphatic chain.

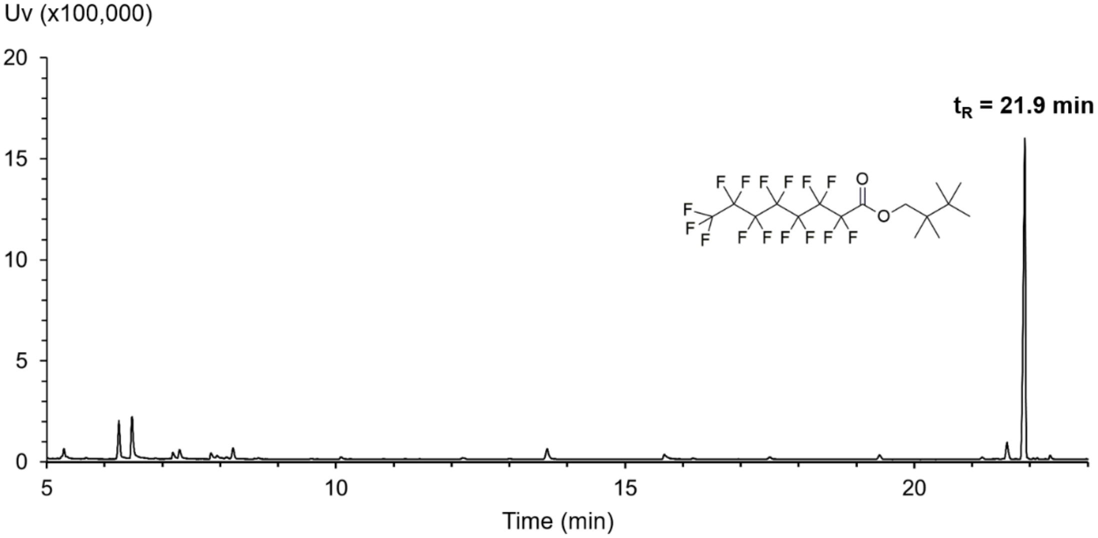

Figure S6. Gas chromatogram with annotated peak of a sample taken after 2 h in the Pt^{II}-catalyzed oxidation of 2,2,3,3-tetramethylbutane in a perfluorinated micro-emulsion. Conditions: 2,2,3,3-tetramethylbutane (0.67 M), K_2PtCl_4 (1 mol%), H_2SO_4 (0.33 M), PFOA (0.48 M), H_2O (1.5 mL), 2 h, 150 °C, 20 bar O_2.

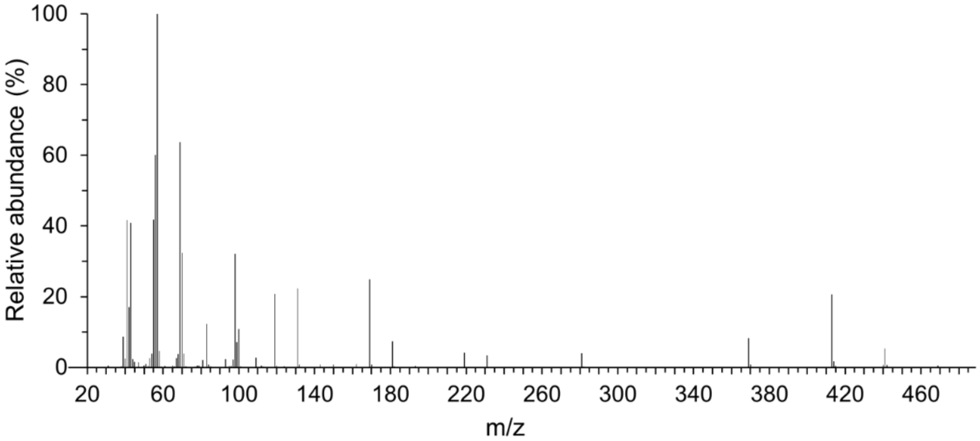

Figure S7. Mass spectrum of 2,2,3,3-tetramethyl-1-butyl perfluorooctanoate; m/z calcd. for $C_{16}F_{15}H_{17}O_2$+• = 526 [M+•]; m/z 441 (5%), 413 (21), 369 (8), 281 (4), 231 (), 219 (4), 181 (7), 169 (25), 131 (22), 119 (21), 98 (32), 83 (12), 70 (32), 69 (64), 57 (100), 56 (60), 55 (42), 43 (41), 41 (42).

4 Structure of the active Pt^{II} catalyst

a) Influence of adding sulfuric acid

Previous findings in Shilov-type reactions have already illustrated the importance of introducing sulfuric acid (H_2SO_4), for example, for improving the oxidizing power of O_2, or to positively alter the electrophilicity of Pt^{II} *via* coordination of its weak conjugated base (HSO_4^-).[2,3] By analogy, sulfuric acid might constitute a vital part of the perfluorinated micro-emulsion in establishing the active catalytic system. A kinetic study was therefore performed in acid-free conditions, with specific attention for the positional selectivities within the heptanol fraction, as well as their time-dependent changes. Strikingly, for short reaction times, terminal C–H activation, with 1-heptanol formation, appeared to be significantly more prominent (Figure S8), pointing towards a faster formation of the active Pt^{II} catalyst when sulfuric acid is omitted from the solution.

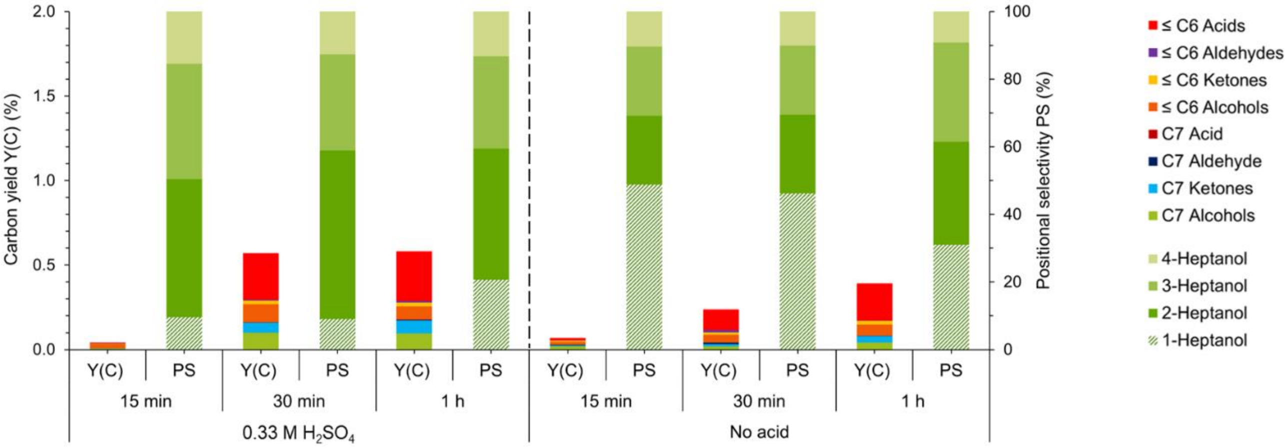

Figure S8. Time profiles for the Pt^{II}-catalyzed oxidation of *n*-heptane in a perfluorinated micro-emulsion, in the presence (left) and absence (right) of sulfuric acid (H_2SO_4). Conditions: *n*-heptane (0.67 M), K_2PtCl_4 (1 mol%), H_2SO_4 (0-0.33 M), PFOA (0.48 M), H_2O (1.5 mL), 0.167-1 h, 150 °C, 20 bar O_2.

b) Role of the perfluorinated micro-emulsion

To provide supporting evidence on the importance of forming a micro-emulsion, a standard reaction was conducted with a surfactant concentration well below the critical micelle concentration (CMC) of PFOA (11 mM at 25 °C and 1 atm);[4] in this way, emulsion formation is prevented as no micelles are available to solubilize *n*-heptane. Figure S9 shows that under such reaction conditions, a significant decline in total product yield occurs, which indicates that the enhanced reaction kinetics in the presence of PFOA can indeed be attributed to the formation of a micro-emulsion system.

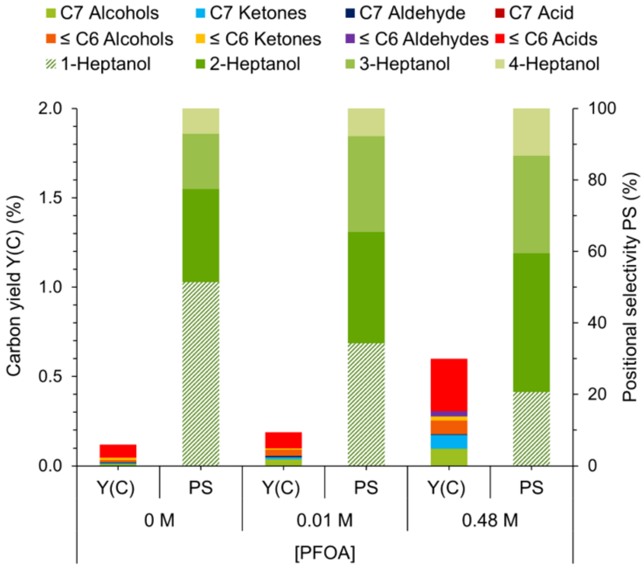

Figure S9. Pt^{II}-catalyzed oxidation of *n*-heptane in a perfluorinated micro-emulsion, with varying concentrations of perfluorooctanoic acid (PFOA). Conditions: *n*-heptane (0.67 M), K_2PtCl_4 (1 mol%), H_2SO_4 (0.33 M), PFOA (0-0.48 M), H_2O (1.5 mL), 1 h, 150 °C, 20 bar O_2.

5 Enhancing the catalytic activity of Pt^{II}

a) Optimization of reactant concentrations

When using a low catalyst loading of 1 mol% K_2PtCl_4, the optimum surfactant concentration was determined to be 0.3 M. Accordingly, with the purpose of promoting the overall activity and taking into account previous findings concerning the detrimental impact of introducing a homogeneous acid, e.g. sulfuric acid, in solution, the catalyst loading was increased in an acid-free micro-emulsion containing 0.3 M of PFOA. As is evident from Figure S10, a remarkable increase in the positional selectivity of 1-heptanol to 60% was obtained by simply doubling the initial concentration of K_2PtCl_4 under these conditions.

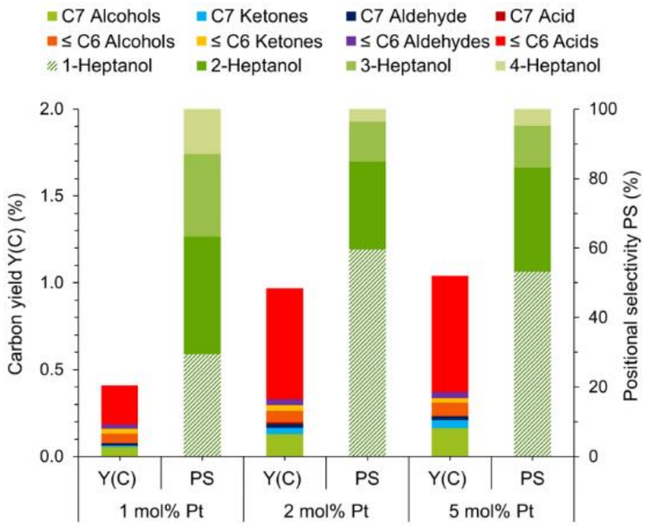

Figure S10. Pt^{II}-catalyzed oxidation of *n*-heptane in an acid-free perfluorinated micro-emulsion containing 0.3 M of PFOA, with varying catalyst loadings. Conditions: *n*-heptane (0.67 M), K_2PtCl_4 (1-5 mol%), PFOA (0.3 M), H_2O (1.5 mL), 1 h, 150 °C, 20 bar O_2.

6 References

1 N. R. Babij, E. O. McCusker, G. T. Whiteker, B. Canturk, N. Choy, L. C. Creemer, C. V. De Amicis, N. M. Hewlett, P. L. Johnson, J. A. Knobelsdorf, F. Li, B. A. Lorsbach, B. M. Nugent, S. J. Ryan, M. R. Smith and Q. Yang, *Org. Process Res. Dev.*, 2016, **20**, 661-667.

2 M. Janssen, L. Van Emelen, C. Marquez, T. De Baerdemaeker and D. E. De Vos, *J. Catal.*¸ 2018, **368**, 345-353.

3 M. Janssen and D. E. De Vos, *Chem. Eur. J.*, 2019, **25**, 10724-10734.

4 H. Hoffmann and J. Würtz, *J. Mol. Liq.*, 1997, **72**, 191-230.